*Heat Transfer 2002, Proceedings of the Twelfth International Heat Transfer Conference,*
*vol. 2, pp. 207-212, 2002*

# Turbulent momentum and heat transfer in ducts of rhombic cross section

Naoya Fukushima and Nobuhide Kasagi

*Department of Mechanical Engineering, The University of Tokyo*
*Hongo 7-3-1, Bunkyo-ku, Tokyo 113-8656, Japan*

**Abstract.** Direct numerical simulation of fully developed turbulent velocity and temperature fields in rhombic ducts with five different acute angles, $\theta$, are carried out. The Reynolds number $Re_b$ based on the bulk mean streamwise velocity and the hydraulic diameter, and the Prandtl number are about 4470 and 0.71, respectively. The mean streamwise velocity and associated mean secondary velocity vectors are obtained at each $\theta$. The systematic change of the secondary flow pattern in the rhombic ducts is clarified. As $\theta$ is decreased, a pair of counter-rotating vortices are distorted near the acute angle corner, and they eventually break up into two pairs at $\theta = 30°$. It is found that the square duct of $\theta = 90°$ gives the best heat transfer performance among the rhombic ducts tested. The dissimilarity between momentum and heat transfer exists and is stronger near the acute corners than near the obtuse ones. This is caused by the dissimilarity inherent in the velocity and thermal boundary conditions, and also by the streamwise velocity decelerated by the corner effect, particularly at the acute corners. For designing thermal mechanical equipment, the duct that has only obtuse corners would be more efficient than that with acute corners.

## 1. Introduction

Turbulent heat transfer is of great importance in a wide range of engineering applications. In many turbomachines and heat exchangers, conduits of various cross sectional shapes are being used to improve the heat transfer and pressure loss. For instance, if we consider a general design strategy of parallel-flow type heat exchangers, its goal would reduce to the optimal partition of the whole cross sectional area of a heat exchanger, where some technologically plausible division shapes should be examined and assessed. They may be *parallel*, *triangular*, *rectangular* and *hexagonal* partitions, which have different apex angles. Given the available pumping power, we should find out the best cross section shape that could achieve the maximum heat exchange. Among feasible shapes, we pay attention to a square and its derivatives, i.e., rhombuses, in the present work.

It is generally known that a solid wall makes Reynolds stresses anisotropic and inhomogeneous through its no-slip and impermeable conditions. In non-circular ducts, anisotropic and inhomogeneous near-wall stresses would then cause secondary flows of the Prandtl's second kind, and consequently alter the turbulence structure. Their effect on momentum and heat transfer is significant. Hence, it is also important to understand the underlying physical mechanism of such wall effects and to develop reliable turbulence models.

Over the decades, a number of numerical and experimental investigations have been carried out to explore the effect of the walls on turbulent flow and temperature fields. However, most of them are concerned with a single plane boundary, which does not involve geometrical complexity such as corners, apexes and wavy walls. Studies on turbulent flow in a non-circular duct are relatively few. For instance, Gavrilakis (1992) and Huser and Biringen (1993) performed direct numerical simulation (DNS, hereafter) of fully developed turbulent flows in a square duct at low Reynolds numbers. They clarified the influence of the duct corner on the stress anisotropy and discussed the origin of the secondary flow. However, there seems to be no literature reporting DNS data of associated turbulent temperature field. As for experimental studies, there are only two on a smooth square duct reported by Brundrett and Burroughs (1967) and Hirota *et al*. (1997), while others seem to have paid more attention to a rough-wall duct. Despite these investigations, the understanding of the effect of the presence of two intersecting walls on turbulent transport mechanism is neither complete nor satisfactory.

From the above background, the basic knowledge on the momentum and heat transfer characteristics of various non-circular conduits is needed. Hence, we study the fully developed turbulent velocity and temperature fields in square and rhombic ducts, where the corners of different angles would cause distinct wall effects.

## 2. Numerical Procedure

The flow geometry and the coordinate system are shown in Fig. 1. The computational details are summarized in Table I. DNS is carried out in five different rhombic ducts. The acute angle $\theta$ is changed from 90 degrees of a square

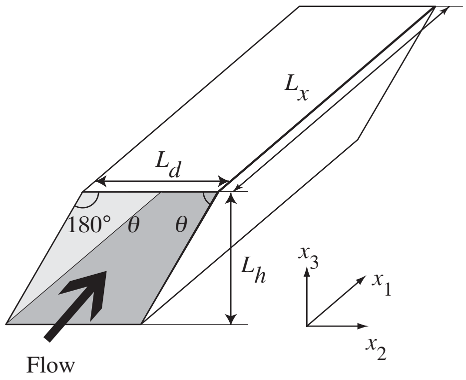


Figure 1 Flow geometry and coordinate system.

duct to 75, 60, 45 and 30 degrees. The computational domain length and the hydrodynamic diameter $D$, i.e., the duct width, $2\delta$, are kept constant. The Reynolds number $Re_b$ based on the bulk mean streamwise velocity $U_b$ and $D$ is set to be about 4470, although a slight difference in $U_b$ exists. The intention to keep $Re_b$ almost constant is that the ratio between the mass flow rate and the wall perimeter length should remain nearly equal for evaluating purely the effect of the cross-section shape on momentum and heat transfer. No-slip condition is imposed on the walls, while the periodic condition is applied at the streamwise boundaries. The time increment is chosen so as to keep the Courant number about 1. The statistics are calculated over the integration time span of about $9000u_\tau^2/\nu$ except for $\theta$= 30, for which the integration is about $6000u_\tau^2/\nu$ because of its heavy computational load. Note that $u_\tau$ and $\nu$ denote the friction velocity and kinematic viscosity, respectively. As shown in Table I, the streamwise and spanwise grid spacings, $\Delta x^+$ and $\Delta d^+$, are about 18 and less than 7, respectively. The latter is made finer than those used in the authors' previous simulation (Fukushima & Kasagi, 2001), because the calculated flow and heat transfer properties in rhombic ducts are found sensitive to the grid refinement. Variables normalized by the wall variables, $u_\tau$, $\nu$ and $T_\tau$ are hereafter denoted by superscript $^+$.

Temperature is considered as a passive scalar with the Prandtl number of the fluid being 0.71. As thermal boundary conditions, the cooling rate is constant along the duct axis with the wall peripheral temperature being constant (Kasagi *et al*., 1992). Thus, the difference between the bulk-mean and wall temperatures is always kept constant. This corresponds to the "thermally thick" wall, of which "dimensionless wall condition parameter," $\phi = k_w t / k_f D$, is infinitely large (Gyves *et al*., 1999) and thermal activity ratio, $K = \sqrt{\left(\rho_f c_{pf} k_f\right) / \left(\rho_w c_{pw} k_w\right)}$, is infinitesimal (Kasagi *et al*., 1989). Here, $k$, $\rho$, $c_p$ and $t$ are the thermal conductivity, the density, the specific heat at constant pressure and the duct wall thickness, with subscripts $w$ and $f$ denoting wall and fluid, respectively.

The Navier-Stokes and energy equations are integrated in time by using the fractional step method (Kim & Moin, 1984). For time advancement, the third-order Runge-Kutta (Spalart *et al*., 1991) and Crank-Nicolson schemes are employed for the advection and viscous terms, respectively. The spatial discretization is made by a second-order finite volume method using a collocated mesh system in the generalized curvilinear coordinate system.

Table I Basic computational conditions.

| | $Re_b$ | $L_x$ x $L_h$ x $L_d$ | $N_x$ x $N_h$ x $N_d$ | $\Delta x^+$ | $\Delta h^+$ | $\Delta d^+$ |
|---|---|---|---|---|---|---|
| Present Study | | | | | | |
| Rhombic ($\theta$ = 90°) | 4477 | 5π x 2 x 2 | 128 x 85 x 85 | 18.65 | 0.196-5.00 | 0.196-5.00 |
| ($\theta$ = 75°) | 4466 | 5π x 2 x 2.07 | 128 x 85 x 85 | 18.59 | 0.194-4.99 | 0.201-5.16 |
| ($\theta$ = 60°) | 4470 | 5π x 2 x 2.31 | 128 x 85 x 85 | 18.34 | 0.191-4.92 | 0.221-5.68 |
| ($\theta$ = 45°) | 4472 | 5π x 2 x 2.82 | 128 x 85 x 85 | 17.79 | 0.186-4.78 | 0.262-6.74 |
| ($\theta$ = 30°) | 4478 | 5π x 2 x 4 | 128 x 107 x 107 | 17.30 | 0.181-3.21 | 0.361-6.42 |

## 3. Results and Discussion

### 3.1 Mean friction and heat transfer properties

The friction factor and the Nusselt number are defined as $f = 8u_\tau^2 / U_b^2$ and $Nu = hD / k_f$, respectively. Their mean values, $f_0$ and $Nu_0$, which have been obtained by averaging local $f$ and $Nu$ over the side length, are given in Table II. In order to compensate a slight difference in the bulk Reynolds numbers among these data, the ratio of $Nu_0/(f_0\,\mathrm{Re}_b)$ is also listed in Table II. For comparison, the DNS result of a circular duct at $Re_b$ = 4300 (Satake *et al*., 2000) is included. All these quantities are also presented as functions of $Re_b$ in Figs. 2(a) and (b), where the Petukhov and Gnielinski empirical equations of $f_p$, $Nu_p$ and $Nu_g$ for a smooth circular duct (Bhatti & Shah, 1987) are compared. In Fig. 2(a), DNS data of $f_0$ in a square duct (Gavrilakis *et al*., 1992; Huser & Biringen, 1993) are also plotted, and it is found that the present value of $f_0$ is very close to the result of Gavrilakis *et al*. (1992).

The friction factor $f_p$ of Petukhov is in good agreement with Satake *et al*. (2000) and also with the experiment of

Table II Comparison of mean flow properties between rhombic and circular ducts.

| | $Re_b$ | $Re_\tau$ | $f_0$ | $Nu_0$ | $Nu_0\,/\,(f_0 Re_b)$ | $U_b$ | $T_b$ | $U_c/U_b$ | $T_c/T_b$ |
|---|---|---|---|---|---|---|---|---|---|
| Present Study | | | | | | | | | |
| Rhombic ($\theta$ = 90°) | 4477 | 304 | 0.0371 | 15.15 | 0.0912 | 14.68 | 14.29 | 1.31 | 1.21 |
| ($\theta$ = 75°) | 4466 | 303 | 0.0369 | 15.00 | 0.0910 | 14.72 | 14.35 | 1.31 | 1.21 |
| ($\theta$ = 60°) | 4470 | 299 | 0.0358 | 14.43 | 0.0901 | 14.94 | 14.72 | 1.32 | 1.22 |
| ($\theta$ = 45°) | 4472 | 290 | 0.0337 | 13.33 | 0.0883 | 15.40 | 15.47 | 1.34 | 1.24 |
| ($\theta$ = 30°) | 4478 | 282 | 0.0318 | 11.73 | 0.0860 | 15.86 | 16.36 | 1.38 | 1.26 |
| Satake *et al*, 2000 | | | | | | | | | |
| Circular | 4300 | 300 | 0.0395 | 15.7 | 0.0924 | 14.75 | | 1.31 | |

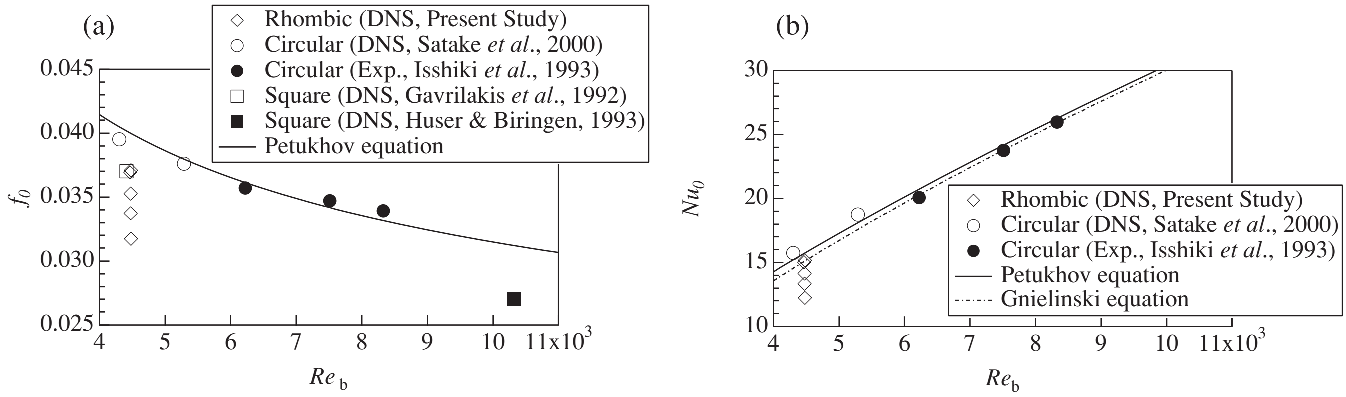


Figure 2 Dependence of a) friction factor $f_0$ and b) Nusselt number $Nu_0$ on bulk Reynolds number, $Re_b$.

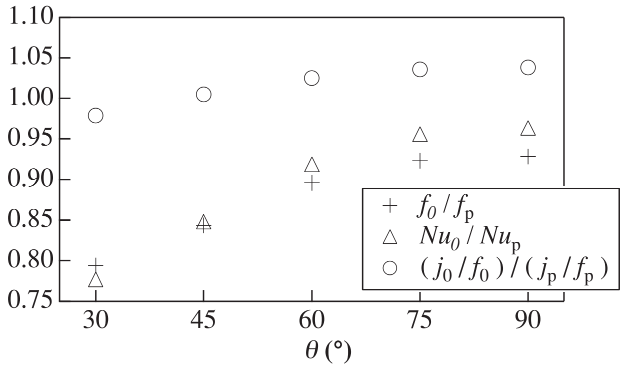


Figure 3 Variation of $f_0\,/\,f_p$ , $Nu_0\,/\,Nu_p$ and $(j_0/f_0)\,/\,(j_0/f_p)$ with $\theta$.

Isshiki *et al.* (1993) in a circular duct, although $f_p$ slightly overpredicts at lower $Re_b$. In Fig. 2(b), the Nusselt umber $Nu_g$ of Gnielinski is in excellent agreement with the experiment at higher $Re_b$, whereas both $Nu_p$ and $Nu_g$ are smaller than corresponding DNS at lower $Re_b$. Especially, $Nu_g$ shows a tendency to underestimate heat transfer in the lower $Re_b$ range. Hereafter, the Petukhov equations are used as a reference.

Comparing $f_0$ and $Nu_0$ in the five different rhombic ducts, it is clear that both values decrease appreciably as the acute apex angle $\theta$ is decreased. Note that $Nu_0$ of a square duct is smaller than that of a circular duct, and this fact is also confirmed in a higher $Re_b$ experiment (Brundrett & Burroughs, 1967). In Fig. 3, the three ratios of $f_0/f_p$, $Nu_0/Nu_p$ and Reynolds analogy factor, $(j_0/f_0)\,/\,(j_p/f_p)$ are shown against $\theta$. Here, $j$ is defined as $St\mathrm{Pr}^{2/3}$. The systematic changes are obvious; $f_0/f_p$ and $Nu_0/Nu_p$ do not change much from $\theta$ = 90° to $\theta$= 75°, but decrease rapidly from $\theta$=75° down to $\theta$=30°. The decrease rate of $f_0/f_p$ is smaller than that of $Nu_0/Nu_p$, so that $(j_0/f_0)\,/\,(j_p/f_p)$ also decreases with $\theta$. Note that the values of $(j_0/f_0)\,/\,(j_p/f_p)$ at $\theta$= 90° and 75° are slightly smaller than and almost equal to that in a circular duct at $Re_b$ = 4300 and 5286, respectively.

Three other heat transfer performance indicators for compact heat transfer surface configurations have separately been compared between five rhombic ducts; that is, the volume $(f\,Re_b/j^2)$ and the total heat transfer area $(f^{1/2}\,/j^{3/2})$ at a constant pumping power $PP$ and a constant number of transfer units $N_{tu}$; and $N_{tu}$, which is equivalent to $(j/(fRe_b^{\,2}))$, at constant $D$ and $PP$ (Cowell, 1990). All indicators show the same tendency that the square duct, $\theta$ = 90°, should give the best performance among the present five rhombic ducts in terms of heat transfer augmentation.

## 3.2 Mean velocity and temperature fields

Rhombic duct flows are characterized by the existence of a pair of counter-rotating vortices, i.e., the secondary flow of the Prandtl's second kind at each corner in the cross stream plane. Figures 4(a)-(e) illustrate the variation of the mean secondary velocity vectors at different acute angles, $\theta$. These vectors have been obtained by averaging over time, streamwise direction and all quarters. It is well known that in the square duct ($\theta = 90°$), a pair of vortices appear in every corner because of the duct symmetry as shown in Fig. 4(a). The centers of vortices in the present study are slightly closer to the corner than those in Gavrilakis *et al*. (1992).

As can be seen in Figs. 4(a)-(e), the configuration of symmetric counter-rotating vortices in the square duct has been replaced by those of non-symmetric skewed vortices in the rhombic ducts. Near the corners of acute angle, a pair of distorted counter-rotating vortices appear with their centers located further away from the corner as $\theta$ is decreased. They eventually break up into two pairs at $\theta= 30°$, the centers of which are located around $x_2/\delta = 1.45$ and 2.35. On the other hand, near the corners of the obtuse angle, there appear a pair of somewhat smaller, but more circular counter-rotating vortices, of which the centers are closer to the corner. The maximum secondary velocity near the acute angle corners is larger than that near the obtuse angle corners. However, the vortices near the acute corners can not intrude deep into the corner. These facts imply that the enhancement of turbulent heat and momentum transfer by the secondary flow is stronger near the obtuse corners than near the acute ones.

The magnitude of the maximum secondary velocity is about 2% of the bulk mean velocity $U_b$ in all ducts tested. It occurs near the vortices closest to the acute angle corners on the corner bisectors except for the square duct, in which it appears near the wall between the corner bisector and the wall bisector. The maximum value is 2.03% of $U_b$ and slightly larger than 2.00% on the corner bisector. In the rhombic ducts, the maximum values are 2.04%, 2.17%, 1.83% and 1.93% of $U_b$ at $\theta = 75°$, 60°, 45° and 30°, respectively. The value on the corner bisector once increases from $\theta = 90°$ to 60°, decreases from $\theta = 60°$ to 45°, and then increases at $\theta = 30°$, where a vortex pair breaks up into two as mentioned above.

The effects of these secondary flows on the mean streamwise velocity, $U/U_b$, and the mean temperature field, $T/T_b$, are shown in Figs. 5(a)-(e). These values have also been averaged over time, streamwise direction and all quarters. Since the induced secondary flow transports efficiently high-momentum and high-temperature fluid from the center to the corner of the duct, the contours of both $U/U_b$ and $T/T_b$ are distorted accordingly. The distortion of $T/T_b$ contours is somewhat smaller than that of $U/U_b$. Similar phenomena have also been observed in the experiment of a square duct at a higher Reynolds number by Hirota *et al*. (1997). These results suggest that the enhancement of heat transfer by the secondary flow is weaker than that of momentum transport. As the acute intersecting angle becomes smaller, the deformation of $T/T_b$ appears more smaller than that of the $U/U_b$. The difference, however, can hardly be found near the obtuse corner.

### 3.3 Local friction and heat transfer characteristics

The distributions of local friction factor and Nusselt number are represented in Fig. 6(a), where both are non-dimensionalized by the values of the Petukhov correlation and plotted against the distance from the acute angle corner, $x_2/\delta$. The considerable decrease of $f/f_p$ and $Nu/Nu_p$ near the acute angle corner with the decrease of $\theta$ is found. This

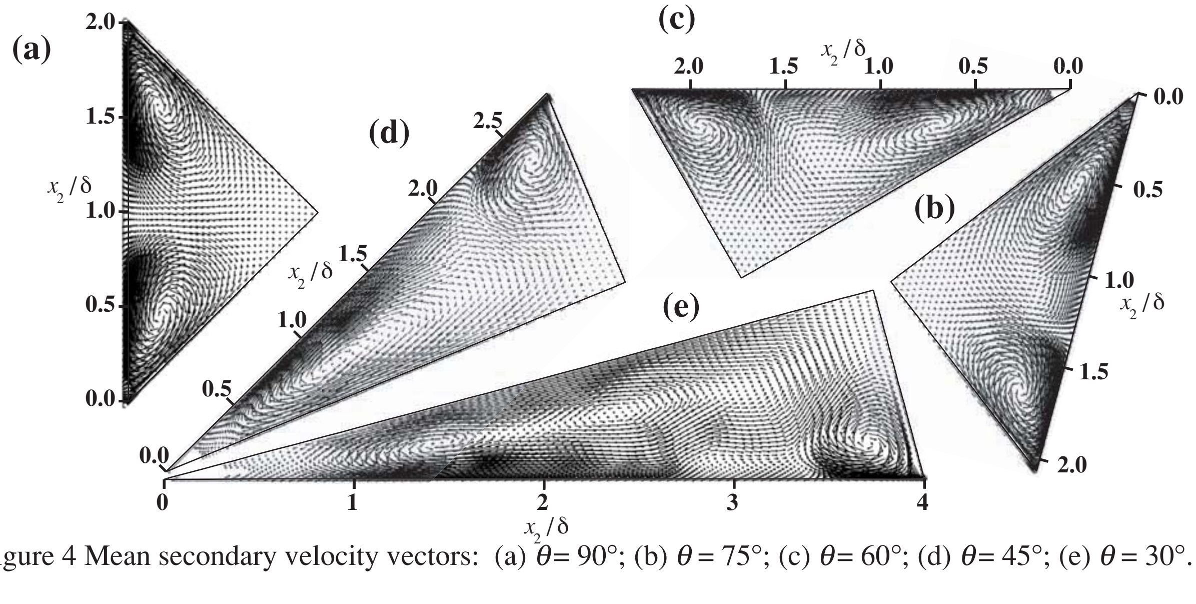


Figure 4 Mean secondary velocity vectors: (a) $\theta= 90°$; (b) $\theta = 75°$; (c) $\theta= 60°$; (d) $\theta= 45°$; (e) $\theta = 30°$.

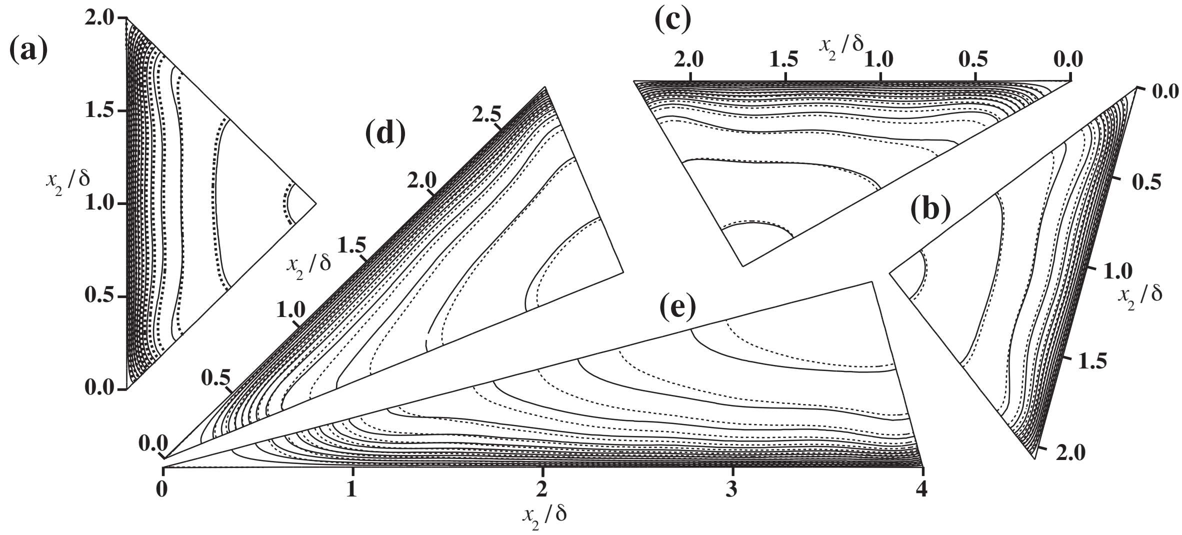


Figure 5 Contours of mean streamwise velocity, $U / U_b$, and mean temperature, $T / T_b$. The contour increments are 0.1 for both $U/U_b$ (solid lines) and $T/T_b$ (dotted lines) with their highest values of 1.3 and 1.2, respectively. (a) $\theta$= 90°; (b) $\theta$ = 75°; (c) $\theta$= 60°; (d) $\theta$= 45°; (e) $\theta$ = 30°.

results in $f_0$ and $Nu_0$, which are smaller in the rhombic ducts with smaller $\theta$. Thus, near the acute angle corners, the enhancement of momentum and heat transfer by the secondary flow should not be superior to the corner suppression effects of Reynolds stresses and turbulent transport.

The dissimilarity between local momentum and heat transfer in five types of rhombic ducts is illustrated in Fig. 6(b), where $(j/j_p) / (f/f_p)$ has a plateau near unity. There is small variation in this value, i.e., 1.06 in the square duct, 1.05 in the circular duct at $Re_b$ = 5286 (Satake *et al*., 2000), and 1.09 in the rhombic duct of $\theta$= 30°. Although the value near the obtuse angle corner approaches a constant value asymptotically, it decreases markedly near the acute angle corner. This implies that the net enhancement of heat transfer by the secondary flow is achieved near the obtuse corners, but not near the acute corners.

Finally, the effect of the thermal boundary condition is considered. In the present study, an axially constant heat-transfer rate per unit length with a constant peripheral wall temperature is assumed. This boundary condition can be interpreted such that temperature is driven by a force, the distribution of which in the cross stream plane is equal to that of the streamwise velocity (see, e.g., Kasagi *et al*., 1992). Note this velocity is driven by the pressure gradient, which is almost uniform in the cross stream plane. These facts result in inferior heat transfer properties near acute angle corners, where the streamwise velocity is much decelerated.

In order to confirm the above hypothesis, additional DNS (on a coarse grid) is carried out in the square duct with the above thermal boundary condition and also with a different boundary condition that heat is generated uniformly in fluid and removed from walls (Kim & Moin, 1989). The latter ideal boundary condition is analogous to that for the velocity field, although it is not realistic. As a result, with the new thermal boundary condition, the dissimilarity between momentum and heat transfer appears less, and $Nu_0$ becomes slightly larger (~1%) . This suggests that the dissimilarity is mostly attributed to the difference in the boundary conditions for the velocity and temperature fields.

From a viewpoint of heat transfer equipment design, it is generally concluded that ducts which have only obtuse angle corners should be more efficient than those with acute angle corners. For example, a hexagonal duct with only obtuse corners may give better heat transfer properties than a circular duct.

## 4. Conclusions

We have simulated the fully developed turbulent velocity and temperature fields in five types of rhombic ducts with acute angles of $\theta$= 90, 75, 60, 45 and 30 degrees to examine the effects of walls on momentum and heat transfer. The thermal boundary condition is given as an axially constant heat-transfer rate per unit length with constant peripheral wall temperature.

The square duct with $\theta$=90° gives the best heat transfer performance among the five rhombic ducts tested. The symmetric counter-rotating vortices in the square duct are replaced by the non-symmetric skewed vortices in the rhom-

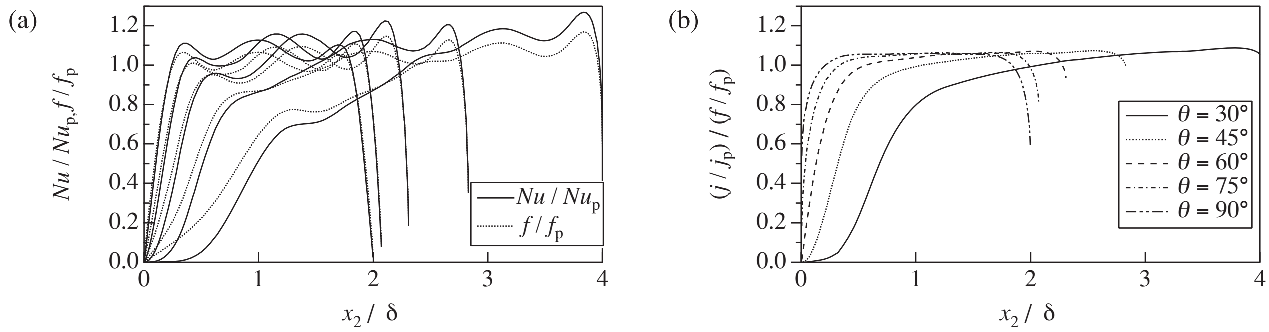


Figure 6 (a) Distribution of local friction factor, $f / f_p$, and local Nusselt number, $Nu / Nu_p$; (b) the ratio between $j / j_p$ and $f / f_p$.

bic ducts. Near the corners of acute angle, a pair of distorted counter-rotating vortices appear. Those vortices are even more strongly distorted and finally break up into two pairs in the duct of $\theta = 30°$. Near the obtuse corners, however, there appear somewhat smaller counter-rotating vortex pairs. As a result, both friction factor and Nusselt number in the rhombic duct become smaller with smaller $\theta$. Thus, the enhancement effect of the secondary flow is not more than the suppression effect of the acute angle corner.

The dissimilarity between momentum and heat transfer exists and is stronger near the acute corners than near the obtuse ones. This is caused by the dissimilarity inherent in the velocity and thermal boundary conditions with the streamwise velocity decelerated by the corner effect, particularly at the acute corners. For designing thermal mechanical equipment, the duct that has only obtuse corners would be more efficient than that with acute corners.

**Acknowledgments**

This work was supported through the research project on "Micro Gas Turbine/Fuel Cell Hybrid-Type Distributed Energy System" by the Department of Core Research for Evolutional Science and Technology (CREST) of the Japan Science and Technology Corporation (JST).

**References**

**journal articles**

Brundrett, E., and Burroughs, P. R., The temperature inner-law and heat transfer for turbulent air flow in a vertical square duct, Int. J. Heat and Mass Transfer. vol. 10, pp. 1133-1142, 1967.

Cowell, T. A., A general method for the comparison of compact heat transfer surfaces, ASME J. Heat Transfer, vol. 112, pp. 288-294, 1990.

Gavrilakis, S., Numerical simulation of low-Reynolds-number turbulent flow through a straight duct, J. Fluid Mech., vol. 244, pp. 101-129, 1992.

Gyves, T. W., Irvine, Jr., T. F. and Naraghi, M. H. N., Gravitational and centrifugal buoyancy effects in curved square channels with conjugated boundary conditions, Int. J. Heat and Mass Transfer, vol. 42, pp. 2015-2029, 1999.

Hirota, M., Fujita, H., Yokosawa, H., Nakai, H. and Itoh, H., Turbulent heat transfer in a square duct, Int. J. Heat and Fluid Flow, vol 18, pp. 170-180, 1997.

Huser, A. and Biringen, S., Direct numerical simulation of turbulent flow in a square duct, J. Fluid Mech., vol 257, pp. 65-95, 1993.

Isshiki, S., Obata, T., Kasagi, N. and Hirata, M., An experimental study on heat transfer in a pulsating flow (1st report, time-averaged turbulent characteristics), Bulletin JSME, vol. 59, pp. 2245-2251, 1993.

Kasagi, N., Kuroda, A., and Hirata, M., Numerical investigation of near-wall turbulent heat transfer taking into account the unsteady heat conduction in the solid wall. ASME J. Heat Transfer, vol. 111, pp. 385-392, 1989.

Kasagi, N., Tomita, Y., and Kuroda, A., Direct numerical simulation of passive scalar field in a turbulent channel flow. ASME J. Heat Transfer, vol. 114, pp. 598-606, 1992.

Kim, J. and Moin, P., Application of a fractional-step method to incompressible Navier-Stokes equations, J. Comp. Phys., 59, pp. 308-323, 1985.

Spalart, P. R., Moser, R. D. & Rogers, M. M., Spectral methods for the Navier-Stokes equations with one infinite and two periodic directions, J. Comp. Phys., 96, pp. 297-324, 1991.

**proceedings**

Fukushima, N. and Kasagi, N., The effect of walls on turbulent flow and temperature fields, Proc. the UEF Conference on Turbulent Heat Transfer III, Girdwood, Alaska, March 2001.

Satake, S., Kunugi, T. and Himeno, R., High Reynolds number computation for turbulent heat transfer in a pipe flow. Proceedings of the 3rd ISHPC, LNCS 1940, M. Valero *et al*., eds., Springer-Verlag, Berlin, pp. 514-52, 2000.

**edited books**

Bhatti, M. S. and Shah, R. K., Turbulent and transition flow convective heat transfer in ducts, Handbook of single-phase convective heat transfer, S. Kakaç, R. K. Shah and W. Aung eds., John Wiley & Sons, New York, pp. **4**-1 - **4**-166

Kim, J. and Moin, P., Transport of passive scalars in a turbulent channel flow, Turbulent Shear Flows VI, J. -C. Andre et al., eds., Springer-Verlag, Berlin, pp. 85-96, 1989.